A Robust Volumetric Feature Extraction Approach for 3D Neuroimaging Retrieval

Sidong Liu[1], Weidong Cai[1], *Member IEEE*, Lingfeng Wen[1,2], *Member IEEE*, Stefan Eberl[1,2], *Member IEEE*, Michael J Fulham[1,2,3], Dagan Feng[1,4] , *Fellow IEEE*

[1] Biomedical and Multimedia Information Technology (BMIT) Research Group, School of Information Technologies, University of Sydney, Australia
[2] Department of PET and Nuclear Medicine, Royal Prince Alfred Hospital, Sydney, Australia
[3] Sydney Medical School, University of Sydney, Australia
[4] Centre for Multimedia Signal Processing (CMSP), Department of Electronic & Information Engineering, Hong Kong Polytechnic University, Hong Kong

***Abstract*— The increased volume of 3D neuroimaging data has created a need for efficient data management and retrieval. We suggest that image retrieval via robust volumetric features could benefit managing these large image datasets. In this paper, we introduce a new feature extraction method, based on disorder-oriented masks, that uses the volumetric spatial distribution patterns in 3D physiological parametric neurological images. Our preliminary results indicate that the proposed volumetric feature extraction approach could support reliable 3D neuroimaging data retrieval and management.**

I. Introduction

NEUROIMAGING has broadened and extended our understanding of how the brain and mind functions and is indispensable for the diagnosis and management of neurological disorders. Neuroimaging datasets have also markedly increased in volume and complexity in the past decade and with the introduction of hybrid imaging devices such as PET-CT and PET-MR, these neuroimaging datasets pose critical challenges for data assimilation. Already there are large neuroimaging databases that are problematic for rapid image retrieval. Traditional key-word based retrieval methods are subjective, time-consuming and may not able to comprehensively describe the images. Thus content-based image retrieval (CBIR) methods supporting full retrieval by visual content/properties have been developed. Feature extraction forms the basis and the most important component of CBIR methods.

A variety of visual features, such as color, texture, shape and spatial relationships, which have been used in other domains, have been adopted in the medical domain with little alteration [1]. Regular feature extraction techniques may not be applicable to functional images such as PET with inherent lower resolution and lack of structural information when compared to anatomical imaging such as CT. In addition, since functional neuroimaging may reflect metabolic activities of human brain, these general visual feature extraction techniques are unable to capture or extract these physiological parameters. Therefore, specific feature extraction methods for neuroimaging retrieval are crucially needed.

A number of visual and physiological features for neurological images have been introduced in the literatures. Wong *et al.* [2] developed a feature that combined the metabolic counts of glucose consumption with the geometric location information. In a recent study, Batty *et al*. [3] proposed an extraction approach, which integrated region of interest (ROI) based texture features extracted by Gabor filters with a related mean index ratio. Our group has previously reported a retrieval system that used a physiological kinetic feature in conjunction with pixel-wise tissue time activity curve (TTAC) clustering in dynamic brain PET images [4].

All of the above features apply to 2D image datasets. However, increasingly, neurological images are collected in 3D format and these previous techniques do not take advantage of the 3D information. Based on our previous study in [4], we further proposed an approach to use the volumetric information as a feature to extract the functional TTACs with the volumes of interest (VOI) that were segmented from dynamic image datasets [5]. More recently, we designed a 3D-key-plane based volumetric feature extraction approach to take further advantage of the spatial information in 3D images. This approach used a set of key planes extracted from one 3D image at different angles to represent the entire volume to achieve fast indexing and retrieval [6]. A limitation of this approach, however, is that data may be missed if the plane does not capture all the voxels contained in one volume.

In this study, we propose a robust volumetric feature extraction approach that captures the spatial information at voxel level with related physiological parameters. The features were extracted from 3D parametric images by volumetric gray level co-occurrence matrices (GLCM) with disorder-oriented spatial masks. We tested the proposed approach on 144 functional neuroimaging studies of patients with suspected dementia taken in the Royal Prince Alfred Hospital, Sydney. We compared our approach to three other retrieval methods using different features.

This work was supported in part by ARC and PolyU grants.

II. METHOD

Our feature extraction approach has five main stages, as shown in Fig. 1.

A. Physiological Parameter Estimation

To make optimum use of the functional parameters we applied the autoradiographic algorithm [7] in voxel-wise parameter estimation. The autoradiographic algorithm is regularly used in routine clinical neurologic studies because it is simple and fast to construct voxel-wise parametric image with a single static scan and two blood samples to calibrate a population-based input function [8].

B. Functional Mapping

We linked the functional data to anatomical landmarks through spatial normalization to a PET brain template using the SPM2 package (Wellcome Trust Centre for Neuroimaging, London, U.K.) [9], and then labeled the structures according to the Tzourio-Mazoyer atlas [10]. The Tzourio-Mazoyer atlas defines 45 functional regions in each hemisphere, 18 in cerebellum and 8 in the vermis. Fig.1 includes an illustration of this atlas and different volumes are represented by different colors.

C. 3D Disorder-oriented Mask Construction

The Tzourio-Mazoyer atlas which has 116 3D functional regions, noted as $\mathbf{M}_{TM}$, was used to map the functional regions and to help design the 3D disorder-oriented mask (3D-DOM) set for the different types of dementia in the dataset. Different disorders eg. a fronto-temporal dementia (FTD) vs. a posterior cortical dementia such as Alzheimer's disease (AD), have different patterns and $\mathbf{M}_{TM}$ can facilitate the mask design by simply mapping the names of functional regions to their anatomical structures in the brain. Here we defined a set of 3D-DOMs, each corresponding to one disorder, based on the literature and expert clinical knowledge. Assuming n total disorders are being investigated, the following statements are satisfied:

1) 3D-DOM Set = $\{\mathbf{M}_{D1}, \mathbf{M}_{D2}, \ldots, \mathbf{M}_{Di}, \ldots, \mathbf{M}_{Dn}\}$, where $\mathbf{M}$ means mask and $\boldsymbol{D_i}$ means the i^{th} disorder;
2) $\mathbf{M}_{Di} \subset \mathbf{M}_{TM}$, where $\boldsymbol{i} = (\boldsymbol{1}, \ldots, \boldsymbol{n})$.

Each mask contains a subset of all the functional regions defined in $\mathbf{M}_{TM}$. As a result, non-relevant regions can be filtered out by applying a mask and the dimensions of the image can also be reduced. For example, the 3D-DOM of AD constructed in this stage includes the posterior cingulate gyrus, precuneus, frontolateral regions, basal forebrain, temporo-parietal association cortices, hippocampus, posterior parietal cortices and posterior inferior temporal areas [11-15], while the FTD mask contains prefrontal cortex, frontal lobes, medial frontal lobe, fronto-lateral and temporal regions, middle temporal gyrus, insula, inferior frontal gyrus, medial frontal gyrus, the basal ganglia and the thalami [11, 16-17].

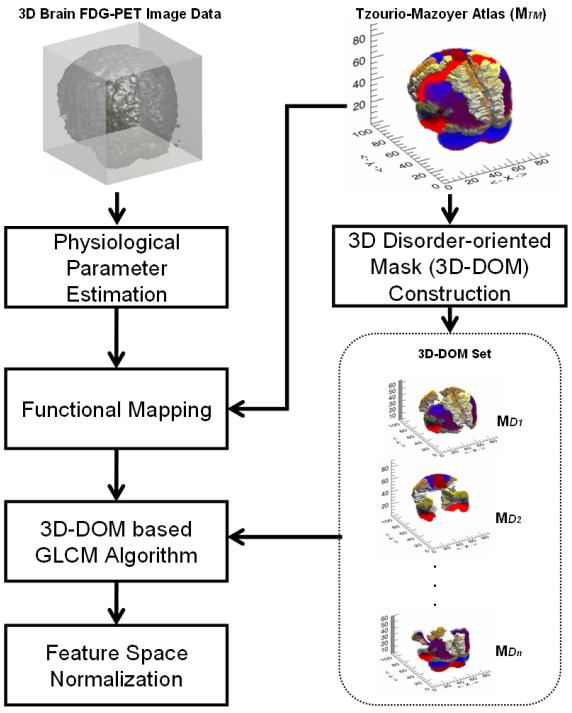

Fig. 1 The framework of our new feature extraction approach.

D. 3D-DOM based GLCM Algorithm

In this stage, 3D-DOMs were applied to all the 3D parametric images, thus all the voxels not covered by the 3D-DOMs were assigned to zero and were not counted when calculating the feature vectors. The localized texture features were extracted from the parametric images filtered out with 3D-DOM by the volumetric GLCM algorithm.

The original GLCM algorithm [18] is widely used in texture analysis because it captures the spatial dependence of gray scale values in an image. A 2D GLCM is an $n \times n$ matrix, where n indicates the number of gray levels representing the image. The value $P[i, j]$ in the matrix captures the counts or probability of pixel pairs having the intensity values i and j. Pixel pairs are defined by a distance d and direction θ, meaning the displacement between this pixel pair happens at d step and θ angle. In general, four directions are defined in 2D GLCM and 14 second order feature descriptors are computed as a set of texture features.

The 2D GLCM algorithm is not able to describe the pixel pair displacements in 3D images. Therefore, we built our approach on the GLCM for volumetric data [19], which are capable of capturing the spatial relationships of voxel intensity values across multiple 3D planes. Every voxel except those on the surface layer of the volume has 26 neighbors. Thus the displacements between the centre voxel and its neighbors can be represented by 26 vectors specified by a distance d and two angles θ and φ, where θ indicates the angle along Z axis and φ means the angle along X axis. Because the displacements are bidirectional, 13 directions are enough to describe the data with no

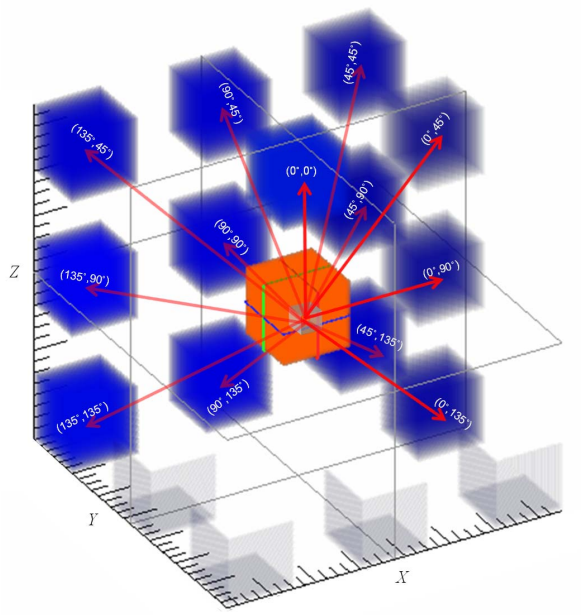

Fig. 2 The 3D illustration of the displacement vectors in 13 directions specified by θ and φ.

redundancy. Fig. 2 illustrates the 13 directions.

To improve the computation efficiency, the number of gray levels to represent the image was binned to 16. Eleven Haralick feature descriptors were implemented: the *Energy*, *Entropy*, *Contrast*, *Variance*, *Correlation*, *Difference Entropy*, *Difference Variance*, *Inverse Difference Moment*, *Sum Entropy*, *Sum Variance* and *Sum Average*.

E. Feature Space Normalization

These 11 feature descriptors had very different ranges for their values. The purpose of feature space normalization is to eliminate the range disparity between different feature spaces and measure similarity on the same basis. Our normalization method took two steps. First, the top 5% of the distribution within each feature space was eliminated, because these extreme values most likely resulted from noise. Second, all the values within the feature space were divided by the nominal maximum of the rest of the 95% elements. The Euclidean distance was used to measure the similarity between two feature vectors.

III. Evaluation

To make our comparison fair between the 3D GLCM approaches and 2D approaches, the same distances of steps (1, 3, 5) were applied in each direction. This ensured that no other factors would affect the accuracy of the retrieval results except the approaches themselves. We also eliminated the discrepancy between the number of 2D GLCM and that of 3D GLCM for one single subject. If one patient's image contains m planes and 12 GLCM (in 4 directions and 3 steps) from each plane are extracted, then there are $m\times12$ matrices for one patient. The value of m may vary according to different 3D-DOMs applied. However, for the 3D GLCM approach, a fixed number (in this study the number was 39, 13 directions with 3 steps each) of matrices were extracted from one patient regardless of the total number of slices or pixels contained in that 3D image. For the 2D methods, the feature vector for one subject was the average value of all the $m\times12$ GLCM of all the planes. As for 3D methods, the feature vector was the average value of all the 39 vectors extracted from the 3D volumetric image.

Further, a comparison between retrieval by the whole brain based feature and by the DOM based feature was also conducted to evaluate the effectiveness of the proposed DOM.

The patient datasets, shown in Table I, were acquired on a CTI ECAT 951R whole body PET scanner, at the Department of PET and Nuclear Medicine, Royal Prince Alfred Hospital. For this study, we used the diagnosis from the patients' reports and the conclusion from the imaging study. A notable feature is that "AD/DLBD" cases refer to those patients categorized as 'indefinite' because there were patterns of glucose hypometabolism consistent with AD and Diffuse Lewy Body Disease (DLBD).

The retrieval was conducted by the *leave-one-out* strategy on the whole dataset. The top ten retrieval results were counted for each query. The relevance criteria were defined as follows. If the retrieval image belongs to the class of the query image, then the relevance score is 1.0. For AD/DLBD cases, if the retrieval image belongs to either AD or DLBD, the score is 0.75. If the retrieval image belongs to any disorder class other than the classes it belongs or relates to, the score is 0.25. If the retrieved image belongs to normal class, the score is 0.

TABLE I
SUMMARY OF THE DATASETS OF PATIENTS WITH SUSPECTED DEMENTIA

Disorder Type	Cases (Male : Female)	Age Range
AD	38 (17:21)	51-73
FTD	37 (21:16)	53-74
AD/DLBD	12 (5:7)	55-73
Other Disorders	39 (20:19)	50-75
Normal	18 (11:7)	53-75
Total	**144 (74:70)**	**50-75**

IV. Results and Discussion

Our approach was compared to three other methods: (1) 3D whole brain based method (3D-WB); (2) 2D whole brain based method (2D-WB); and (3) 2D-DOM based method. Fig. 3 and Fig. 4 show the comparisons between retrieval results of these four methods for three disorders.

From the figures, we see that the precisions of the two 2D GLCM methods are very similar and there are only slight improvements (0.4% to 4.2%) in the 2D-DOM based method. The reason is that 2D GLCM methods adopted a plane-based averaging mechanism which decreases the significance of affected regions, since it was undermined by the larger area of unaffected regions.

The retrieval results of 3D GLCM methods, meanwhile, had a much broader and more inclusive range than the 2D methods and the improvement by applying masks is

striking (14.5% higher for AD and 11.6% higher for FTD compared with 3D-WB). These findings may be explained by: 1) The 3D methods may alleviate the effect of DOMs even more extensively than the 2D counterparts since these 3D approaches construct GLCM on all the voxel elements in the whole volume, while the 2D methods build up GLCM only based on the cross-planes; 2) The 3D approaches capture the 3D spatial distribution traits, which is beyond the capability of the 2D methods. The 3D-WB method suffers more from the offset of an overwhelmingly large amount of non pathological voxels, while the DOM based approach benefits from the ability to capture perceivable characteristics of voxel distributions. Therefore, the 3D-WB approach has a lower precision than the 2D approaches, but the 3D-DOM approach produces more accurate results.

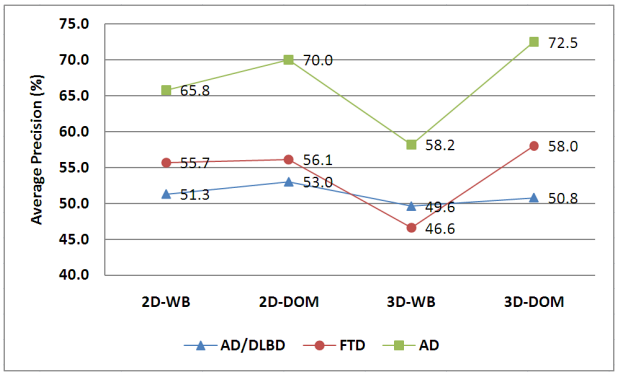

Fig. 3 The comparison of retrieval results for three disorders (AD/DLBD, FTD, AD).

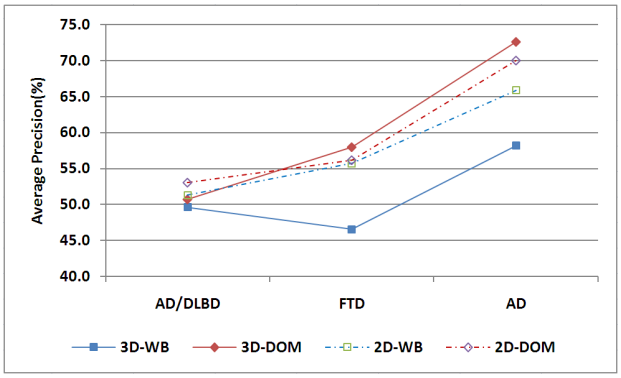

Fig. 4 The comparison of retrieval result by the proposed 3D-DOM based approach and other three approaches.

V. Conclusions

In this work, we present a new volumetric feature extraction approach for 3D neuroimging retrieval. Our preliminary data suggest that our proposed approach is a robust tool for volumetric texture feature extraction and the disorder-oriented masks facilitate and improve the retrieval of 3D functional neuroimaging datasets. The framework of our feature extraction approach is well defined, more disorders and other features will be investigated in our future work.

References

[1] H. Muller, N. Michoux, D. Bandon, and A. Geissbuhler , "A review of content-based image retrieval systems in medical applications – clinical benefits and future directions," *International Journal of Medical Informatics*, vol. 73, pp.1-23, 2004.

[2] S.T.C. Wong, K.S. Hoo, X. Cao, *et al*., "A neuroinformatics database system for disease-oriented neuroimaging research," *Academic Radiology*, vol. 11, no. 3, pp. 345-358, 2004.

[3] S. Batty, J. Clark, T. Fryer, and X. Gao, "Prototype system for semantic retrieval of neurological PET images," presented at 2nd Int. Conf. on Medical Imaging and Informatics (MIMI 2007), Beijing, Aug 14-16, 2007, LNCS 4987, pp. 179-188.

[4] W. Cai, D. Feng and R. Fulton, "Content-Based Retrieval of Dynamic PET Functional Images," *IEEE Trans. on Information Tech. in Biomedicine*, vol. 4, no. 2, pp.152-158, 2000.

[5] J. Kim, W. Cai, D. Feng, and H. Wu, "A new way for multi-dimensional medical data management: volume of interest (VOI)-based retrieval of medical images with visual and functional features," *IEEE Trans. on Information Tech. in Biomedicine*, vol. 10, no. 3, pp.598-607, 2006.

[6] W. Cai, S. Liu, L. Wen, S. Eberl, M.J. Fulham and D. Feng, "3D neurological image retrieval with localized pathology-centric CMRGlc patterns," *The Int. Conf. on Image Processing (ICIP 2010)*, submitted for publication.

[7] G.D. Hutchins, J.E. Holden, R.A. Koeppe, *et al.*, "Alternative approach to single-scan estimation of cerebral glucose metabolic rate using glucose analogs with particular application to ischemia," *J. of Cereb. Blood Flow and Metab.*, vol. 4, pp. 35-40, 1984.

[8] S. Eberl, A.R. Anayat, R. Fulton, P.K. Hooper, and M.J. Fulham, "Evaluation of two population-based input functions for quantitative neurological FDG PET studies," *European J. of Nuclear Medicine,* vol. 24, no. 3, pp. 299-304, 1997.

[9] R. S. J. Frackowiak, K. J. Friston, C. D. Frith, *et al*., *Human Brain Function*. Amsterdam; Boston: Elsevier Academic Press, 2004.

[10] N. Tzourio-Mazoyer, B. Landeau, *et al.*, "Automated Anatomical Labeling of Activations in SPM Using a Macroscopic Anatomical Parcellation of the MNI MRI Single-Subject Brain," *NeuroImage,* vol. 15, no. 1, pp. 273-289, 2002.

[11] M. Brand, and H. J. Markowitsch, "Brain Structures Involved in Dementia," in *Competence Assessment in Dementia*. New York: Springer-Vienna, 2008, pp. 25-34.

[12] N. Kerrouche, K. Herholz, R. Mielke, *et al.*, "18 FDG PET in vascular dementia: differentiation from Alzheimer's disease using voxel-based multivariate analysis," *J. Cereb. Blood Flow Metab.*, vol. 26, no. 9, pp. 1213-1221, 2006.

[13] L.A. van de Pol, A. Hensel, W.M. van der Flie, *et al.*, "Hippocampal atrophy on MRI in frontotemporal lobar degeneration and Alzheimer's disease," *J. Neuro. Neurosurg. Psychiatry*, vol. 77, no. 4, pp. 439-442, April 1, 2006.

[14] A. Brun, and L. Gustafson, "Distribution of cerebral degeneration in Alzheimer's disease," *European Archives of Psychiatry and Clinical Neuroscience*, vol. 223, no. 1, pp. 15-33, 1976.

[15] S. Teipel, J. Pruessner, F. Faltraco et al., "Comprehensive dissection of the medial temporal lobe in AD: measurement of hippocampus, amygdala, entorhinal, perirhinal and parahippocampal cortices using MRI," *J. of Neurology*, vol. 253, no. 6, pp. 794-800, 2006.

[16] J. Slowinski, A. Imamura, R.J. Uitti, *et al.*, "MR imaging of brainstem atrophy in progressive supranuclear palsy," *Journal of Neurology*, vol. 255, no. 1, pp. 37-44, 2008.

[17] B. Ibach, S. Poljansky, J. Marienhagen *et al*., "Contrasting metabolic impairment in frontotemporal degeneration and early onset Alzheimer's disease," *NeuroImage*, vol. 23, no. 2, pp. 4, 2004.

[18] R. M. Haralick, K. Shanmugam, I. Dinstein, "Texture features for image classification," *IEEE Trans. Sys., Man., and Cyb.*, vol.SMC-3, no. 6, 1973.

[19] S. Kurani, D.H. Xu, J. Furst, and D.S. Raicu, "Co-occurrence matrices for volumetric data," in *Proc. 7th Int. Conf. on Computer Graphics and Imagine (CGIM)*, Hawaii, 2004.